

## THE STOPPING POWER AND RANGE OF ENERGETIC PROTON BEAMS IN NICKEL TARGET RELEVANT FOR COPPER-64 PRODUCTION

Imam Kambali, Hari Suryanto and Herlan Setiawan  
Center for Radioisotopes and Radiopharmaceuticals Technology (PTRR), BATAN  
Kawasan Puspiptek Serpong, Tangerang Selatan, Indonesia  
Email: imamkey@batan.go.id

### ABSTRACT

**THE STOPPING POWER AND RANGE OF ENERGETIC PROTON BEAMS IN NICKEL TARGET RELEVANT FOR COPPER-64 PRODUCTION.** The energy loss distribution of a range of energetic proton beams in nickel (Ni) target has been simulated using the Stopping and Range of Ion in Matter (SRIM 2013) codes. The calculated data of the proton's range would then be used to determine the optimum thickness of Ni target for future production of  $^{64}\text{Cu}$  radioisotope. In general, the stopping power and range of proton beam in Ni depend strongly on the proton energy and incidence angle. It was also found that for an incidence angle of  $0^\circ$  with respect to the target normal, the best thickness of a Ni target should be between 260 – 350  $\mu\text{m}$  for proton energy between 10 – 12 MeV. Furthermore, the thickness should be decreased with increasing incidence angle for optimum  $^{64}\text{Cu}$  radioactivity yield. The case study on the production of  $^{64}\text{Cu}$  by a 15.5-MeV proton bombardment indicated that the lower-than-expected yield was most likely due to a thinner Ni target than it should have been.

**Keywords:** stopping power, range, proton beam, Ni target,  $^{64}\text{Cu}$  production

### ABSTRAK

**KAJIAN TERHADAP DAYA HENTI DAN JANGKAUAN PROTON DI DALAM TARGET NICKEL DAN RELEVANSINYA UNTUK PRODUKSI RADIOISOTOP TEMBAGA-64.** Distribusi energi yang hilang dari sejumlah berkas proton berenergi tinggi telah disimulasikan menggunakan program *Stopping and Range of Ion in Matter* (SRIM 2013). Hasil data perhitungan jangkauan proton tersebut selanjutnya akan digunakan untuk menentukan ketebalan optimum target Ni untuk produksi radioisotop  $^{64}\text{Cu}$  di masa yang akan datang. Secara umum, daya henti dan jangkauan proton sangat tergantung pada energy dan sudut datang berkas proton. Untuk sudut datang  $0^\circ$  (tegak lurus terhadap permukaan target), ketebalan optimum target nikel direkomendasikan sebesar 260 – 350  $\mu\text{m}$  jika target tersebut diiradiasi dengan berkas proton berenergi antara 10 – 12 MeV. Selain itu, ketebalan tersebut hendaknya dikurangi jika berkas proton ditembakkan dengan sudut yang lebih besar dari  $0^\circ$  untuk optimasi hasil radioaktivitas  $^{64}\text{Cu}$ . Studi kasus terhadap produksi  $^{64}\text{Cu}$  dengan proton berenergi 15,5 MeV menunjukkan bahwa hasil radioaktivitas yang lebih rendah dari perhitungan teori kemungkinan besar disebabkan oleh target Ni yang terlalu tipis.

**Katakunci:** daya henti, jangkauan, berkas proton, target Ni, produksi  $^{64}\text{Cu}$ .

**INTRODUCTION**

Cyclotron-produced radionuclides such as <sup>18</sup>F, <sup>123</sup>I and <sup>11</sup>C have been widely used and developed for Positron Emission Tomography (PET) in domestic [1] and overseas hospitals [2,3], whereas an intermediate-lived radionuclide such as <sup>64</sup>Cu is still under developing as potential radiotherapy reagents [4,5]. Copper-64 can be produced in a cyclotron by accelerating a proton beam up to a certain energy level before being irradiated into a highly-enriched <sup>64</sup>Ni target via a nuclear reaction <sup>64</sup>Ni(p,n)<sup>64</sup>Cu. The resulting <sup>64</sup>Cu radioisotope has a half-life of 12.7 hours and emission characteristics of <sup>-</sup> (38%), <sup>+</sup> (19%) and Electron Capture (43%) [6]. However generating <sup>64</sup>Cu at a desired level of radioactivity is not an easy task since the radioactivity yield depends strongly on the Ni target thickness, cross sections of the nuclear reaction and some other technical parameters [7]. In addition, the nuclear cross section is also dependent of the proton beam energy as shown in **Fig. 1**, which indicates that the optimum proton energy for the <sup>64</sup>Ni(p,n) <sup>64</sup>Cu nuclear reaction is around 10 – 11 MeV [8,9].

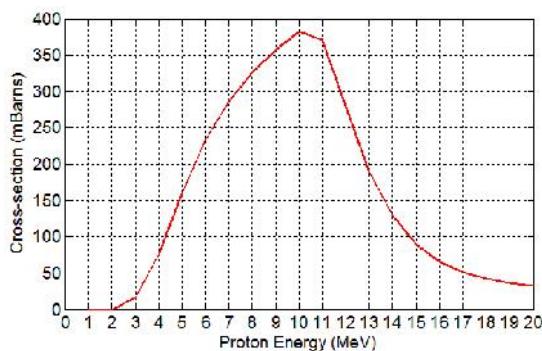


**Fig. 1** TALYS-Calculated excitation function of <sup>64</sup>Ni(p,n)<sup>64</sup>Cu nuclear reaction [8].

Another important parameter relevant to the <sup>64</sup>Cu production is the target thickness as it corresponds to the radioactivity yield. Knowledge

about proton distributions in the Ni target is, therefore, paramount to successfully determine the correct target thickness prior to proton irradiation. The proton distributions in Ni target can be examined from the particle’s stopping power/energy loss and range, which can be calculated using Stopping and Range of Ion in Matter (SRIM) package [10]. In the SRIM codes, stopping power is defined as the energy required to slowing down the incident particle during its interaction with matter over a certain distance, and is mathematically expressed as [11]:

$$S(E) = -\frac{dE}{dx} = \frac{4\pi k_0^2 z^2 e^4 n}{mc^2 \beta^2} \left[ \ln \frac{2mc^2 \beta^2}{I(1-\beta^2)} - \beta^2 \right] \dots\dots\dots (1)$$

Where  $k_0 = 8,99 \times 10^9 \text{ N.m}^2.\text{C}^2$ ,  $z$  = atomic number,  $e$  = charge of electron,  $n$  = number of electron per unit volume of the target,  $m$  = mass of electron at rest,  $c$  = speed of light in vacuum,  $\beta$  = ratio of the speed of the incident particle to the speed of light,  $I$  = average excitation energy of the target.

After losing energy and reaching a maximum stopping power (called Bragg peak) due to nuclear and electronic interactions, the incident ion will eventually stop at a certain distance from the target surface and leave some vacancies in the target. The distance over which the ion totally stops is called the projected range  $R(E)$ , which satisfies [11]:

$$R(E) = \int_0^E \frac{1}{(-\frac{dE}{dx})} dE \dots\dots\dots (2)$$

Paul [12] has recently compared the stopping power of some experimental data to the SRIM-calculated results and to a few other available software for a number of incident ions ranging from hydrogen to uranium. Moreover, in most cases he found that the SRIM-calculated results best fit the experimental data. Another earlier studies [13] also

used SRIM package to calculate the range of several proton beams in pure water relevant for  $^{18}\text{F}$  production.

This paper reports on the use of the SRIM codes to discuss the stopping power and range of proton in Ni target and employ the calculated data to determine the optimum thickness of the Ni target for  $^{64}\text{Cu}$  radioisotope production. The dependence of the range, and hence, the optimum target thickness on the proton beam incidence angle are also examined. In addition, a case study on the effect of setting up an incorrect thickness of Nickel target to the  $^{64}\text{Cu}$  radioactivity yield is also presented.

## THEORETICAL CALCULATIONS

The theoretical calculations of the stopping power and range of several energetic proton beams of up to 30 MeV in Ni target (99.99%-enriched  $^{64}\text{Ni}$ ) were carried out using the SRIM 2013 version codes. For some expected proton energy (10, 11 and 12 MeV) for optimum  $^{64}\text{Cu}$  radioisotope production, the angle of incidence was also varied from  $\theta = 0^\circ$  to  $\theta = 70^\circ$  with respect to the Ni target normal (as defined in **Fig. 2**).

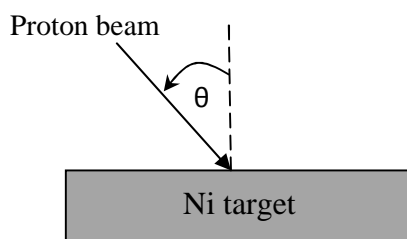


**Fig. 2** Proton beam and Ni target set-up in the SRIM calculations

In every investigated proton energy, there were nearly 100,000 protons simulated in the calculations. As well, a 15.5 MeV proton beam was simulated for the purpose of a case study based on a paper written

by McCarthy, *et al* [14] to explain why they obtained much lower  $^{64}\text{Cu}$  radioactivity yield in their experiments than they had expected in the theory.

## RESULTS AND DISCUSSION

### Stopping Power and Range of Energetic Proton Beams in Ni Target

An example of the longitudinal and lateral distributions of a 5-MeV proton beam bombarded into a 100- $\mu\text{m}$  thick Ni target can be seen in **Fig. 3**, in which around 99.9% of the incident proton hit the target and stop after passing through a distance of nearly 80  $\mu\text{m}$ . Around 0.1% of the incident proton is scattered off the target atoms at an angle of less than  $90^\circ$ , but there are no backscattered ions observed in the simulation.

The behavior of the proton beam distributions in the energy range between 5 MeV and 30 MeV is relatively similar which can be inferred from the shape of their energy loss/stopping power plots (**Fig. 4**). In general, for any proton energy, the stopping power increases with increasing distance of travel until it peaks at a certain value (called Bragg peak) and then drops dramatically following the loss of the proton energy. In contrast to the general trend of the energy loss, in which it decreases with increasing proton energy, the range increases with increasing proton energy as shown in the inset of **Fig. 4**. The range goes up quite steeply from 73.8  $\mu\text{m}$  at proton energy of 5 MeV to 154  $\mu\text{m}$  for the 30-MeV proton beam, whereas there are 47 target atoms displaced by the incoming 5 MeV proton beam compared to 137 vacancies as a result of the 30-MeV proton irradiation.

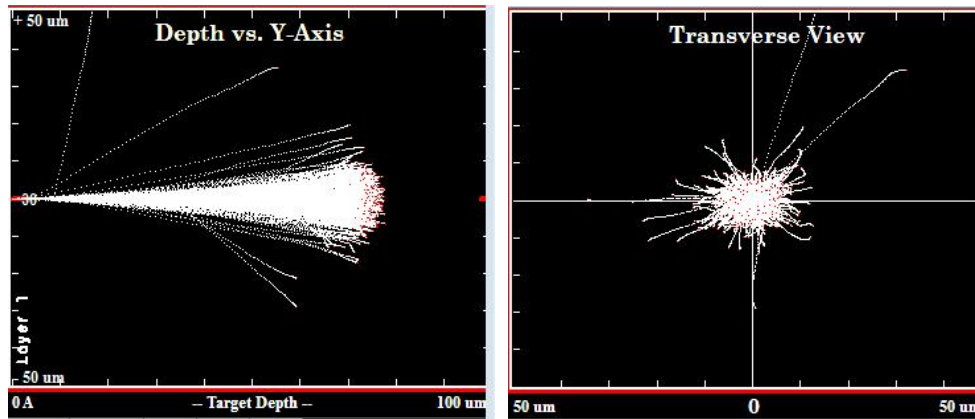


**Fig. 3** Trajectories of a 5-MeV proton beam in nickel target calculated using the SRIM 2013 version package [10], depicted from longitudinal (left) and transversal (right) views .

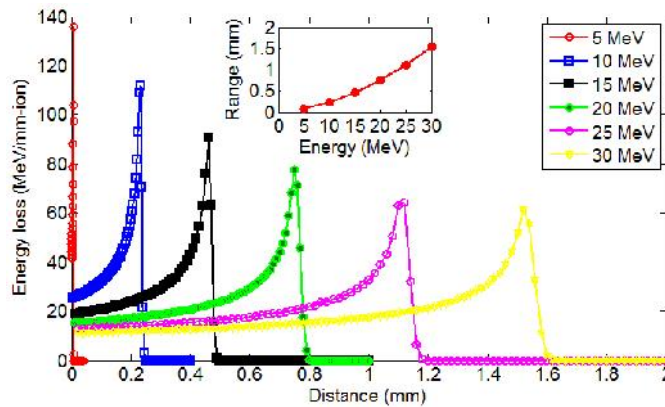


**Fig. 4** Energy loss of several energetic proton beams ranging from 5 MeV to 30 MeV in nickel target, calculated using the SRIM 2013 version package [10]. The corresponding ranges are shown in the inset.

### Angle Dependence of Proton Range

The following section discusses the dependence of the proton range on the incidence angle for proton energy of 10, 11 and 12 MeV. The 3 energy regimes were chosen in conjunction with the optimum cross-section for  $^{64}\text{Ni}(p,n)^{64}\text{Cu}$  nuclear reaction (see **Fig. 1**). For a beam of 10-MeV

protons, the larger the incidence angle the shorter the distance it travels, which is due to higher stopping power as depicted in **Fig. 5**. In other words, the range of the proton is shorter as the incidence angle increases (**inset, Fig. 5**). It is also clear that the distribution of the energy loss broadens with increasing incidence angle.

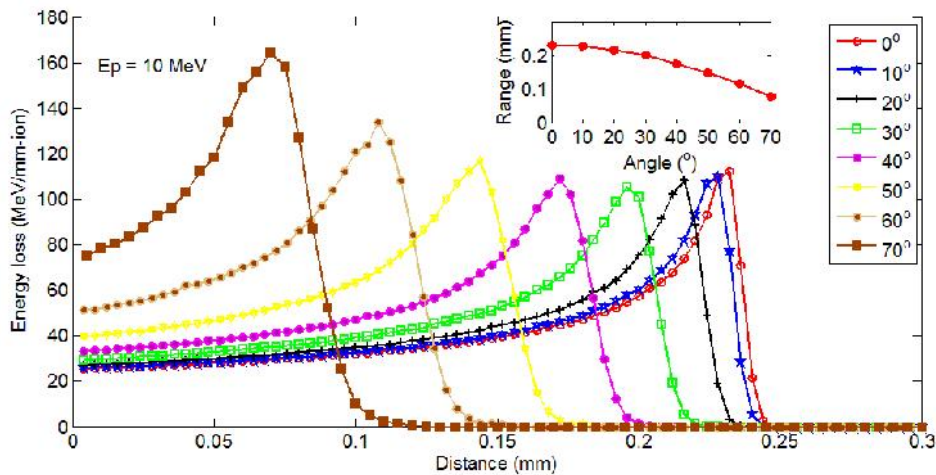


**Fig. 5** Stopping power and range (inset) of a 10-MeV proton beam in Ni target at various angles of incidence

The behavior of the stopping power, range and ion distribution is relatively similar for the two other proton energy (11 MeV and 12 MeV) investigated in this study. Again, the projected range of the three simulated proton energy drop when the proton incidence angles increase, whereas, in contrast, the lateral range is larger with bigger angle (**Fig. 6**). Furthermore, at an incidence angle of 48°, for all proton energy, the projected range reaches exactly the same value as their respective lateral range. Increasing the incidence angle further will result in longer lateral range as compared to the projected range.

### Recommended Ni Thickness for Optimum <sup>64</sup>Cu Production

As discussed elsewhere, Nickel target can be made by electroplating technique [14-16], or prepared as a foil target [17] and possibly by plasma deposition. Regardless of the methods used for the Ni target preparation, it is important to know the best

thickness for optimum <sup>64</sup>Cu radioactivity yield. Based on the SRIM calculations, the recommended thickness of Ni target appropriate for the PET radioisotope production is summarized in Table 1. Note that the recommended thicknesses were derived from the calculated range of proton beams at 10, 11 and 12 MeV, plus a 10% increase from their original values to compensate deviation which maybe encountered experimentally.

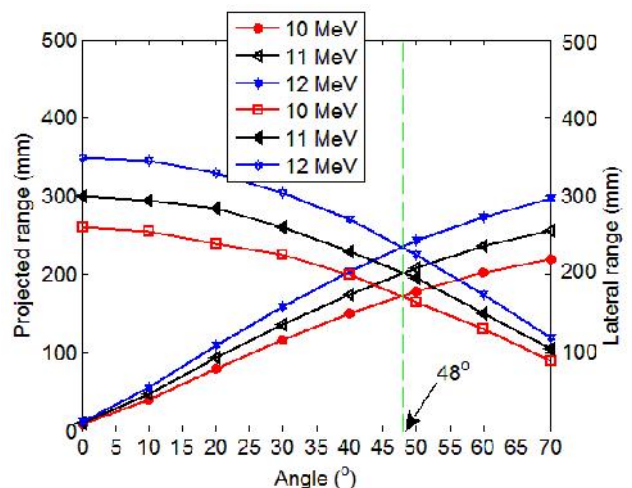


**Fig. 6** Ranges of 10-12 MeV proton beams in Ni target at various angles of incidence.

**Table 1** Recommended thicknesses of Nickel targets for 3 different proton energies as a function of angle of incidence

Angle of incidence (degrees)	Ni thickness ( $\mu\text{m}$ )		
	$E_p = 10 \text{ MeV}$	$E_p = 11 \text{ MeV}$	$E_p = 12 \text{ MeV}$
0	260	300	350
10	255	295	345
20	240	285	330
30	225	260	305
40	200	230	270
50	165	195	225
60	130	150	175
70	90	105	120

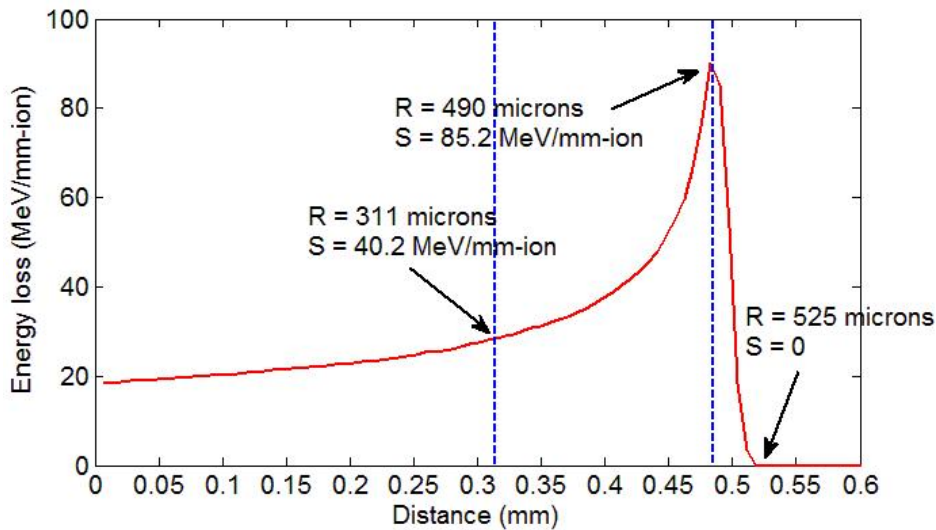


**Fig. 7** Stopping power of a 15.5-MeV proton beam in Ni target simulated using SRIM package.

For a 10-MeV proton beam, for instance, the best thickness for Ni target is suggested around 260  $\mu\text{m}$ ; however the thickness shall be increased to 350  $\mu\text{m}$  when the energy is increased to 12 MeV. In addition, the target should be tilted to a larger angle relative to the incoming beam for a thinner target. This general rule also applies to higher proton energy.

**A Case Study: Incorrect Thickness Results in Low Yield**

This case study is based on a paper written by McCarthy, *et al* [14] in which they irradiated

enriched  $^{64}\text{Ni}$  targets with a 15.5-MeV proton beam to produce  $^{64}\text{Cu}$  radioisotope. In one of their experiments, the Ni target was prepared by electroplating to create some 311  $\mu\text{m}$ -thick Ni films plated on a gold substrate. With this experimental set-up, the predicted End-Of-Bombardment (EOB) yield should be around 10.5 mCi/ $\mu\text{A}\cdot\text{hr}$ ; however they only obtained approximately 5 mCi/ $\mu\text{A}\cdot\text{hr}$ . While they argued that the lower-than-expected EOB yield might be due to the Ni target misalignment, we offer and examine 2 other possible explanations here, i.e:

(1) Low cross-section regime.

As widely reported elsewhere [8,9], the maximum cross-section for  $^{64}\text{Ni}(p,n)^{64}\text{Cu}$  nuclear reaction is around 10 – 11 MeV, and therefore any  $^{64}\text{Cu}$  production using proton as the incident beam should be carried out around those values. However in the McCarthy, *et al* [14] experimental case, they bombard the electroplated Ni target using a 15.5 MeV proton beam which is much higher than the optimum energy required to get optimum EOB yield. Since the radioactivity yield is directly proportional to the excitation function/cross-section [7], and also since the cross-section of the  $^{64}\text{Ni}(p,n)^{64}\text{Cu}$  nuclear reaction at 15.5 MeV is nearly a factor of 7 lower than that of at 10 MeV, this may explain why their experimental set-up yielded much lower EOB activity than the theory.

(2) Thin Ni target.

Based on the SRIM-calculated data, a 15.5 MeV proton beam is able to penetrate relatively deep into a Ni target and pass the target after losing its total energy. The average range of such an energetic proton beam is about 490  $\mu\text{m}$ , whereas its total range is nearly 525  $\mu\text{m}$  (Fig. 7). Again, the optimum yield at this particular proton energy would only be obtained if the Ni target thickness was around 525  $\mu\text{m}$ . However in the case of McCarthy, *et al* investigation [14], they employed a 311- $\mu\text{m}$  thick Ni target to produce  $^{64}\text{Cu}$ , which is too thin to totally stop the incoming 15.5-MeV proton beam. At a distance of 311  $\mu\text{m}$  from the Ni surface, the protons would lose nearly half of its energy; hence, a vast number of protons would pass through the

thin Ni target and deposit only a few fraction of their total energy. Therefore, the proton-bombarded Ni target in their experiment results in much lower-than expected EOB. However if the theoretical yield was presumably calculated at the experimental proton energy – hence, the proper cross-section –, we favor the second explanation.

## CONCLUSION

Knowledge about stopping power and range of proton in Ni target is essential to better understand the behavior of the particle's distribution in the target for  $^{64}\text{Cu}$  production. The thickness of Ni target for any energetic proton irradiated on the target can be estimated using its stopping power and range. For instance, for a 10 MeV incoming proton beam, the Ni target thickness required to fully stop the beam without being able to escape the target's rear surface is about 260  $\mu\text{m}$ . Optimum thicknesses for certain proton incidence angles and energies are also reported in this paper. A serious mistake related to the Ni film thickness chosen as an appropriate target for  $^{64}\text{Cu}$  production could happen if there is not proper information on the range of proton in the Ni target as discussed in the study case section of this paper. This typical mistake could result in a much-lower-than expected  $^{64}\text{Cu}$  radioactivity. Future work will concentrate on the theoretical  $^{64}\text{Cu}$  radioactivity yield from proton-irradiated  $^{64}\text{Ni}$  targets.

## ACKNOWLEDGEMENTS

The writers acknowledge the Indonesian National Nuclear Energy Agency (BATAN) for financially supporting this research program. Meaningful discussion with Mr. Rajiman and Serly A. Sarungallo is also greatly appreciated.

## REFERENCES

1. LISTIAWADI F D., HUDA N, SURYANTO H., PARWANTO., "Produksi radionuklida Fluor-18 untuk Penandaan Radiofarmaka 18FDG Menggunakan Siklotron *Eclipse* di Rumah Sakit Kanker Darmais". Prosiding Pertemuan dan Presentasi Ilmiah Teknologi Akselerator dan Aplikasinya, Oktober 2013, Vol. 1 (2013) 1-4.
2. SHARP S E., SHULKIN B L., GELFAND M J., *et al*, "<sup>123</sup>I-MIBG Scintigraphy and <sup>18</sup>F-FDG PET in Neuroblastoma", J. Nucl. Med. 50(8) (2009) 1237-1243.
3. ZANZONICO P., "Positron Emission Tomography: A Review of Basic Principles Scanner Design and Performance, and Current Systems", Seminars in Nuclear Medicine, Vol XXXIV, No 2 (2004) 87-111.
4. MATARRESE M., BEDESCHI P., SCARDAONI R., *et al*, "Automated production of copper radioisotopes and preparation of high specific activity [<sup>64</sup>Cu] Cu-ATSM for PET studies". Appl. Radiat. Isot. 68 (2010) 5–13.
5. ACHMAD A., HANAOKA H., YOSHIOKA H., *et al*. "Predicting cetuximab accumulation in KRAS wild-type and KRAS mutant colorectal cancer using <sup>64</sup>Cu-labeled cetuximab positron emission tomography". Cancer. Sci. 103 (2012) 600–605.
6. LEDERER C M and SHIERLEY V S., (1978). Table of Isotopes, 7th edn. MacMillan, New York.
7. LEPERA C G., "PET Radionuclides Production Cyclotron Selection and Location, Cyclotopes and Experimental Diagnostic Imaging, The University of Texas MD Anderson Cancer Center Houston, TX.  
aapm.org/meetings/08SS/documents/Gonzalez.pdf. Retrieved on 10 March 2013.
8. KONING A J., ROCHMAN D., MARCK S V D., *et al*, "'TENDL-2013: TALYS-based evaluated nuclear data library" , www.talys.eu/tendl-2013.html. Retrieved on 10 March 2014.
9. LEDERER C M and SHIERLEY V S., (1978). Table of Isotopes, 7th edn. MacMillan, New York.
10. ZIEGLER J F., ZIEGLER M D and BIRSACK J P., "SRIM – The Stopping and Range of Ions in Matter (2010)", Nucl. Inst. Meth. Phys. Res. B 268 (2010) 1818–1823.
11. ZIEGLER J F., BIRSACK J P AND ZIEGLER M D., (2008). "Stopping and Range of Ions in Matter". SRIM Co., Chester, MD.
12. PAUL H., "Comparing experimental stopping power data for positive ions with stopping tables, using statistical analysis", Nucl. Inst. Meth. Phys. Res. B 273 (2012) 15–17.
13. KAMBALI I., HERYANTO T., RAJIMAN., ICHWAN S., "Reliability Study of the Liquid Target Chamber for <sup>18</sup>F Production at the BATAN's Cyclotron Facilities", Atom Indonesia 37 (1) (2011) 5 – 10.
14. MCCARTHY D W., SHEFER R E., KLINKOWSTEIN R E., "Efficient production of high specific activity <sup>64</sup>Cu using a biomedical cyclotron", Nucl. Med. Biol. 24, (1997) 35–43.
15. SOLE V., HOWSE J., ZAW M., *et al*, "Alternative method for <sup>64</sup>Cu radioisotope production", Appl. Rad. Iso. 67 (2009) 1324–1331.
16. OBATA A., KASAMATSU S., MCCARTHY D W., *et al*, "Production of therapeutic quantities of <sup>64</sup>Cu using a 12 MeV cyclotron", Nucl. Medi. Biol. 30 (2003) 535–539.
17. KLINKOWSTEIN R E., MCCARTHY D W., SHEFER R E., WELCH M J., "Production of <sup>64</sup>Cu and other radionuclides using a charged-particle accelerator", US Patent Number US6011825 A (2000).